

SCIENTIFIC REPORTS



OPEN

Predicting influenza antigenicity from Hemagglutinin sequence data based on a joint random forest method

Yuhua Yao¹, Xianhong Li², Bo Liao³, Li Huang⁴, Pingan He⁴, Fayou Wang⁵, Jiasheng Yang⁶, Hailiang Sun⁷, Yulong Zhao⁸ & Jialiang Yang^{1,9}

Timely identification of emerging antigenic variants is critical to influenza vaccine design. The accuracy of a sequence-based antigenic prediction method relies on the choice of amino acids substitution matrices. In this study, we first compared a comprehensive 95 substitution matrices reflecting various amino acids properties in predicting the antigenicity of influenza viruses by a random forest model. We then proposed a novel algorithm called joint random forest regression (JRFR) to jointly consider top substitution matrices. We applied JRFR to human H3N2 seasonal influenza data from 1968 to 2003. A 10-fold cross-validation shows that JRFR outperforms other popular methods in predicting antigenic variants. In addition, our results suggest that structure features are most relevant to influenza antigenicity. By restricting the analysis to data involving two adjacent antigenic clusters, we inferred a few key amino acids mutation driving the 11 historical antigenic drift events, pointing to experimentally validated mutations. Finally, we constructed an antigenic cartography of all H3N2 viruses with hemagglutinin (the glycoprotein on the surface of the influenza virus responsible for its binding to host cells) sequence available from NCBI flu database, and showed an overall correspondence and local inconsistency between genetic and antigenic evolution of H3N2 influenza viruses.

Causing an estimated 500,000 deaths worldwide per year, influenza epidemics in humans seriously endanger population health and world economy¹. Vaccination is the primary option to reduce influenza outbreaks. The efficacy of a seasonal influenza vaccine depends largely on the selection of vaccine strains, i.e., the strains this vaccine is designed to prevent. A good vaccine recipe should target potential circulating strains able to escape from population immunity in the new flu season². However, influenza viruses are classic examples of antigenically variable pathogens and have a seemingly endless capacity to evade immune response³, which makes vaccine design extremely challenging. According to reports from the center for disease control and prevention (CDC), flu shots fail half of the time⁴. As such, timely identification of emerging antigenic variants is critical to influenza vaccine design, flu surveillance, and human health⁵.

One of the most popular assays to evaluate the efficacy of a vaccine against an influenza virus is the hemagglutination inhibition (HI) assay, a binding assay measuring the ability of antisera (vaccine) to block the hemagglutinin (HA) of the antigen (virus) from agglutinating red blood cells⁶. However, HI assay is labor and cost intensive, which poses the need for efficient computational methods to estimate the antigenic similarity between antigens and antisera². With the advances of sequencing techniques, influenza sequences have become more and more

¹School of Mathematics and Statistics, Hainan Normal University, Haikou, 570100, P. R. China. ²College of Life Sciences, Zhejiang Sci-Tech University, Hangzhou, 310018, P. R. China. ³College of Information Science and Engineering, Hunan University, Changsha, 410082, P. R. China. ⁴College of Sciences, Zhejiang Sci-Tech University, Hangzhou, 310018, P. R. China. ⁵School of Mathematics and Information Science, Henan Polytechnic University, Henan, 454000, P. R. China. ⁶Department of Civil and Environmental Engineering, National University of Singapore, Singapore, 119077, Singapore. ⁷College of Veterinary Medicine, Huanan Agricultural University, Guangzhou, 510000, P. R. China. ⁸Department of Mathematics, City University of Hong Kong, Hong Kong, P. R. China. ⁹Department of Genetics and Genomic Sciences, Icahn School of Medicine at Mount Sinai, NY, 10029, USA. Correspondence and requests for materials should be addressed to Y.Z. (email: zhaoyulong@gmail.com) or J.Y. (email: jialiang.yang@mssm.edu)

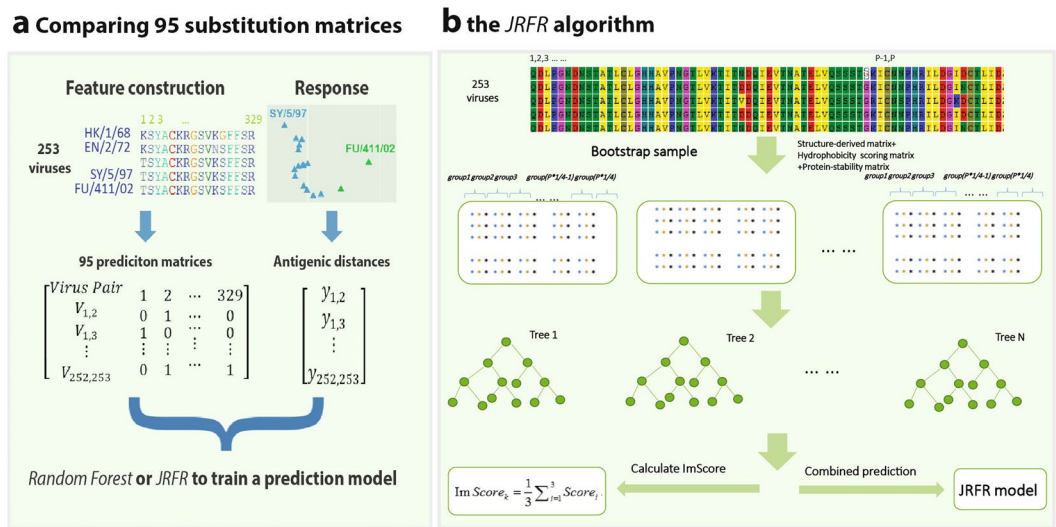


Figure 1. A flowchart to illustrate the computational framework in this study.

available⁷, making them good candidates for predicting the antigenicity of new viruses and identifying antigenic variants.

Popular antigenic prediction methods include imputation-based methods^{5,8}, and sequence-based methods. Sequence-based methods usually associate mutations in HA proteins with antigenic differences (among viruses) obtained from serological tests^{5,8,9}. The antigenic differences are either quantified by antigenic distances⁵ or simply represented by a binary value to indicate if two viruses are antigenic variants^{9,10}. For example, Liao *et al.* tested four algorithms including iterative filtering, multiple regression, logistic regression, and support vector machine to predict antigenic variants from mutations in HA1, a sub-unit of HA forming globular domain¹¹. They also explored six amino acids substitution models based on physicochemical grouping of 20 amino acids¹⁰. Sun *et al.* proposed Antigen-Bridges, a bootstrapped ridge regression model, to predict antigenic distances using amino acids substitutions quantified by pattern-induced multisequence alignment (PIMA) in HA1 protein sequences². As H3N2 influenza viruses from 1968 to 2003 are grouped into 11 antigenic clusters, i.e., HK68, EN72, VI75, TX77, BK79, SI87, BE89, BE92, WU95, SY97, and FU02 in chronological order⁵, they also predicted HA mutations driving antigenic drift events between adjacent clusters and experimentally validated two predicted mutation sets (i.e., from BE92 to WU95 and from WU95 to SY97). Noticing that co-evolution in HA1 might contribute to antigenic evolution, Yang *et al.* developed a Lasso model incorporating both single and co-mutation features in HA1 protein sequences¹². More recently, Qiu *et al.* developed a protein structure-based antigenic prediction model¹³, and Neher *et al.* developed an optimization model to interpret known antigenic data and evaluated its ability in predicting composition of future influenza virus populations¹⁴. There are also many other methods in this hot topic, e.g., Huang *et al.*¹⁵ and Ren *et al.*¹⁶ to name but a few.

Despite the fact that these methods are greatly helpful in selecting antigenic variants and optimizing vaccine strains, there are still a few points to be improved. First, it is known that the scoring matrices to quantify amino acids substitutions are critical to the accuracy of prediction algorithms^{10,13}. However, only a few matrices reflecting partial protein attributes have been tested, e.g., binary substitution matrix¹⁷, physicochemical models¹⁰, PAM250, BLOSUM62, PIMA¹², and structure model¹³. A systematic study of the relationship between amino acids attributes and influenza antigenicity is largely missing. AAindex, a database of numerical indices representing various physicochemical and biochemical properties of amino acids and pairs of amino acids, provides an opportunity to fix this gap¹⁸. The predictive powers of the 94 physicochemical and biochemical properties of amino acids in AAindex could be helpful to elucidate their contribution to influenza antigenic evolution. Second, it is unclear if the combination of a few important amino acids attributes can better predict influenza antigenicity. Third, most previous models either predict antigenic variants or adopt linear models. There might be some advantages in predicting continuous antigenic distances using nonlinear models like random forest¹⁹ since antigenic distances have higher resolution than binary values and the relationship among antigenic sites might be nonlinear.

In this study, we propose and test Joint Random Forest Regression (JRFR), a novel algorithm that combines multiple substitution matrices into the random forest algorithm to predict antigenic distances from HA1 protein sequences. We also systematically compare 95 amino acids substitution matrices in predicting the antigenicity of H3N2 influenza viruses. These substitution matrices reflect a comprehensive list of amino acids attributes including structural, physicochemical, and biochemical information. Finally, we explore the relationship between genetic and antigenic evolution of H3N2 influenza viruses based on the prediction results from JRFR.

Results

JRFR: a random forest model to predict antigenic distances. We illustrated our computational framework in Fig. 1. We trained a predictive model by taking the amino acids' changes among virus pairs at each protein site as a feature and the pairwise antigenic distances among viruses as the response (see Materials and

Accession No	Description	RMSE
NIEK910102	Structure-derived correlation matrix 2	0.965
NIEK910101	Structure-derived correlation matrix 1	0.967
RIER950101	Hydrophobicity scoring matrix	0.968
MIYS930101	Base-substitution-protein-stability matrix	0.968
DOSZ010102	Normalised version of SM_SAUSAGE	0.970
LUTR910102	Structure-based comparison table for inside other class	0.970
AZAE970102	The substitution matrix derived from spatially conserved motifs	0.971
BENS940101	Log-odds scoring matrix collected in 6.4–8.7 PAM	0.972
TUDE900101	isomorphism of replacements	0.973
AZAE970101	The single residue substitution matrix from interchanges of spatially neighbouring residues	0.973
HENS920102	BLOSUM62 substitution matrix	0.986
DAYM780301	Log odds matrix for 250 PAMs	1.000
Binary	1 for substitution and 0 for match	1.098

Table 1. The top 12 amino acids substitution matrices in predicting influenza antigenicity.

Methods for details). There are many amino acids substitution matrices reflecting different attributes of amino acids¹⁸ and the choice of substitution model has been proven to be critical in prediction accuracy^{9, 10, 16}. Thus, we first evaluated the prediction powers of a comprehensive 95 amino acids substitution matrices (i.e, 94 matrices in AAindex¹⁸ and binary substitution one) by applying the random forest algorithm (Fig. 1a). We then proposed the JRFR algorithm by jointly considering 2 or more substitution matrices. Specifically, we first selected the top 15 substitution matrices according to 10-fold cross-validation prediction accuracy, each was considered as a major matrix. The 94 secondary matrices (matrices other than the major matrix) were then selected one by one to join the model in a greedy manor to improve prediction accuracy (see Materials and Methods). The top model was selected for predicting the antigenicity of new influenza viruses. For simplicity, we only allowed at most 2 secondary matrices. Based on the importance score of each protein locus in JRFR, we also evaluated the contribution of a mutation to antigenic change and antigenic drift events.

Evaluation of amino acids attributes in predicting influenza antigenicity. We applied our computational framework into the H3N2 human influenza data from 1968 to 2003⁵, a curated HI table of 253 viruses and 79 vaccines. According to Smith *et al.*⁵ the viruses are classified into 11 antigenic clusters namely HK68, EN72, VI75, TX77, BK79, SI87, BE89, BE92, WU95, SY97, and FU02, respectively. The pairwise antigenic distances among the viruses were calculated based on Metric MDS⁵ and were used as responses in our models. We then downloaded the HA1 protein sequences (of length 329) for the 253 viruses from NCBI flu database⁷, and aligned them using MUSCLE²⁰. The alignment was then transformed into 95 feature matrices based on the 94 amino acids substitution models in AAindex¹⁸ and the binary substitution model. The 10-fold cross-validation root-mean-square errors (RMSEs) for all 95 models were summarized in Supplementary Table S1, among which we listed a few top or well studied models in Table 1.

As can be seen, the selection of substitution models indeed has some influences in prediction accuracy. The best model “Structure-derived correlation matrix 2” has a RMSE 0.965, 15% lower than that of the worst model “Context-dependent optimal substitution matrices for buried coil” (1.111). In Cai *et al.*¹⁷ it was shown that the 10-fold cross-validation RMSEs are 1.051 for their MC-MDS model and 1.047 for Metric MDS model⁵ using the same data. So our best model has 8.5% lower RMSE than both models. Interestingly, the top models are derived from structure-based substitution matrices, implying the importance of HA1 protein structure in influenza antigenicity. It is quite reasonable since antigenicity measures the binding affinity between antigen and antiserum, in which structure information is critical⁶. A few commonly used substitution models including binary (1.098), PAM250 (0.977), and BLOSUM62 (0.986) perform not as good as structure ones. The reason might be that they could not reflect much information related to antigen-antiserum reaction.

Since influenza antigenicity is known to associate with many attributes of HA protein, e.g., structure and hydrophobicity, we conjectured that it might be helpful to combine a few amino acids characteristics. Thus, we also applied our JRFR model by combining multiple substitution matrices. The prediction accuracy is indeed improved by JRFR (see Table 2 for a few top combinations), confirming that influenza antigenicity is affected by many protein attributes. The best combination uses NIEK910101 mutation matrix (“Structure-derived correlation matrix 1”) as the main feature matrix and RUSR970101 (“Substitution matrix based on structural alignments of analogous proteins”) and KOSJ950107 (“Context-dependent optimal substitution matrices for buried turn”) as auxiliary feature matrices. The 10-fold cross-validation RMSE could be reduced to 0.941 (with prediction accuracy 0.963, sensitivity 0.980, specificity 0.775 and the Mathew’s correlation coefficient (MCC) 0.756) by this model. It is of note that the prediction accuracy could be further improved by adding new secondary matrices, however, the improvement is marginal. As such, we adopt the best model with 3 feature matrices for all subsequent analyses.

Main data	Merge data 1	Merge data 2	RMSE	Accuracy	Specificity	Sensitivity	MCC
NIEK910101	RUSR970101	KOSJ950107	0.941	0.963	0.775	0.980	0.756
RIER950101	FEND850101	FEND850101	0.943	0.964	0.777	0.981	0.758
NIEK910101	RUSR970101	None	0.950	0.963	0.767	0.981	0.753
RIER950101	FEND850101	None	0.952	0.963	0.771	0.980	0.753
NIEK910102	RUSR970101	None	0.952	0.963	0.767	0.981	0.754

Table 2. Performances of seven prediction models.

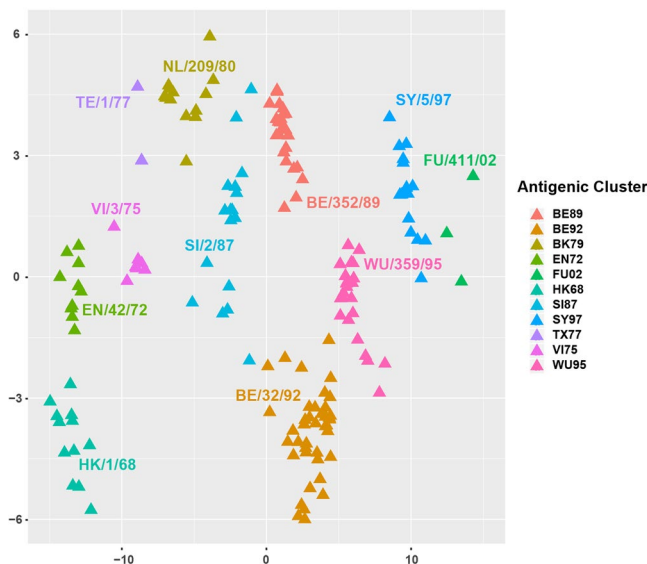


Figure 2. The antigenic map of 253 H3N2 influenza viruses predicted by JRFR. The 11 antigenic clusters HK68, EN72, VI75, TX77, BK79, SI87, BE89, BE92, WU95, SY97, and FU02 are marked by different colors.

Relationship between influenza genetic and antigenic evolution as revealed by JRFR. Based on the antigenic distances inferred by JRFR, we constructed the antigenic cartography of the 253 H3N2 viruses by multidimensional scaling (see Fig. 2). As can be seen from the figure, all the 11 antigenic clusters are well separated. The viruses have been evolving alongside an S-shaped path antigenically. Viruses in a few clusters are more compact (e.g., BE89) while others are more spread (e.g., SI87). Sequence-based antigenic cartography could be useful in selecting potential antigenic variants for further serological test and thus benefits vaccine design².

Since 253 viruses might only represent partial antigenic evolution, we downloaded all 1638 non-redundant H3N2 HA1 protein sequences between 1968 and 2014 from NCBI flu database and predicted their antigenic distance using JRFR. We plotted their genetic and antigenic map (see Materials and Methods) in Fig. 3. As can be seen, the genetic and antigenic maps are generally consistent. However, the genetic map is more continuous while the antigenic map is more punctual. The result is consistent with a few previous studies^{2,5}. To evaluate historical vaccine strains, we marked a few known vaccine strains in both genetic and antigenic maps. We found that some vaccine strains are very close to each other in the genetic map but relative far in the antigenic map. For example, the genetic distance between BE/352/1989 and BE/32/1992 is less than 0.01, however their antigenic distance is larger than 3. Similar scenarios could be found for A/Wisconsin/67/2005 and A/Perth/16/2009. The observation indicates that the contribution of genetic mutation to antigenicity is different at different protein sites. Only a small set of sites might be responsible for antigenic evolution⁵.

Sites driving antigenic changes in H3N2 influenza A viruses. We inferred the antigenic importance of each protein sites by their importance score in the JRFR model. We plotted the log₁₀-transformed importance score for all 329 sites in HA1 protein in Fig. 4 and listed the actual values of the top 34 sites (with log₁₀ importance large than 2.9) in Table 3. It is known that HA consists of five epitopes (epitope A, B, C, D, and E), each having around 20 structural neighbour amino acids locating on the protein surface^{21–23}. A few recent studies experimentally and computationally identified important antigenic sites, most of which locate on the 5 epitopes^{2,12,24,25}. As can be seen from Table 3, vast majority of the key sites are located on the five epitopes^{21–23} especially on epitope A and B. Among the top 34 antigenically important sites, there are 11 in epitope B (i.e., 189, 163, 159, 156, 158, 196, 190, 155, 193, 157, and 197), 8 in A (i.e., 133, 145, 135, 137, 131, 144, 143, and 142), 6 in D (i.e., 173, 226, 248, 121, 217, and 172), 5 in C (i.e., 278, 276, 307, 53, and 299), and 4 in E (i.e., 83, 94, 262, and 62). Interestingly, we also identified an antigenic sites (i.e., 2) not belonging to any epitope, which is consistent with a few previous studies^{2,12}. These sites might be important in driving future antigenic evolution of H3N2 influenza A viruses.

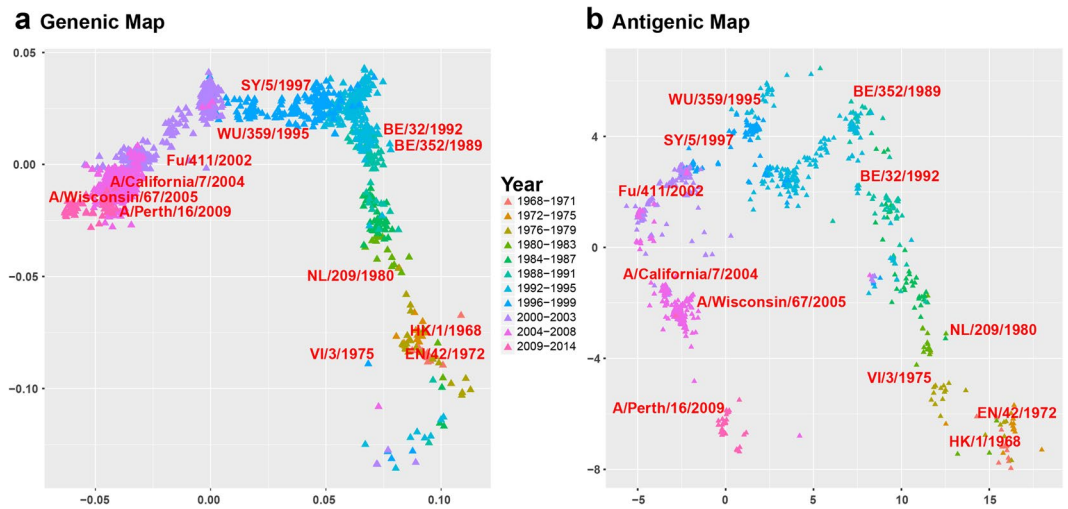


Figure 3. The genetic (a) and antigenic map (b) for all 1968 non-redundant H3N2 HA1 protein sequences between 1968 and 2014. The viruses are colored by their year of discovery.

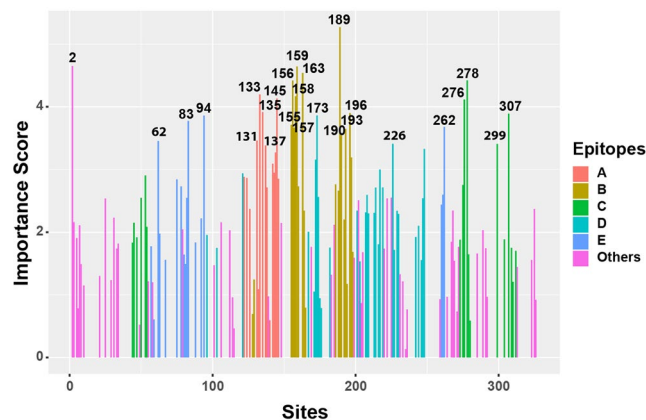


Figure 4. The importance score of all 329 sites predicted by JRFR. The 5 epitopes A, B, C, D, and E are marked in different colors. The remaining sites are classified as “Others”.

Mutations driving H3N2 influenza antigenic drift events. There are 10 antigenic drift events for H3N2 influenza viruses occurred between 1968 and 2003⁵. We also applied JRFR on viruses in chronologically adjacent antigenic clusters to infer amino acids mutations driving specific drift event based on importance scores. The combination of mutations responsible for the 10 drift events were listed in Table 4. Interestingly, we observed a few antigenic sites critical for multiple antigenic drift events. For example, site 193 drove the early two antigenic drift events, i.e., HK68-EN72 and EN72-VI75. Site 145 was involved in 4 antigenic drifts, i.e., EN72-EN75, SI87-BE89, BE89-BE92, and BE92-WU95.

To validate the power of these sites in driving antigenic drift events, we manually selected one virus at the center of one antigenic group, and mutated its amino acids, by which we obtained a few artificial variants of the selected virus. We then predicted the antigenicity of the variants (based on its HA1 sequence) and test if it has similar antigenicity with viruses in the later antigenic group. For a better view, we plotted the antigenic cartography of the viruses in two adjacent antigenic clusters, the selected virus, and its artificial variants (see Fig. 5). We only plotted the late 4 clusters since they have more viruses. As one can see, in most cases the predicted mutation combinations are capable of driving the antigenic drifts. Sun *et al.* experimentally validated that N145K can drive BE92-WU95, which is consistent with our predictions².

Discussion

As we know, the antigenicity of influenza viruses changes rapidly and vaccines should be updated accordingly to avoid influenza outbreaks. The vaccines have been updated at least 27 times for H3N2 viruses since 1968, 9 times for H1N1 virus from 1977 to 2009, and 15 times for influenza B virus from 1972 to 2011². However, the selection of vaccine strains is non-trivial due to the exceptional large number of new influenza viruses in the new season and the burden in testing antigenicity of these virus against known vaccines. As a result, flu shots from CDC fail half the time⁴. Thus, timely surveillance of the antigenic evolution of these viruses is critical. However, traditional experimental methods such as HI assay for evaluating the antigenicity of new viruses face a multitude of issues.

Site	Importance Score	Antigenic Domain	Site	Importance Score	Antigenic Domain
189	5.273	B	262	3.678	E
2	4.651	other	157	3.664	B
159	4.645	B	193	3.646	B
163	4.541	B	190	3.545	B
278	4.421	C	131	3.460	A
156	4.417	B	62	3.453	E
133	4.196	A	226	3.408	D
158	4.167	B	299	3.406	C
145	4.133	A	137	3.383	A
276	4.116	C	248	3.326	D
135	3.915	A	144	3.270	A
196	3.899	B	197	3.189	B
307	3.890	C	172	3.154	D
173	3.862	D	142	3.091	A
94	3.859	E	217	2.998	D
83	3.775	E	143	2.946	A
155	3.712	B	121	2.936	D

Table 3. The top 34 antigenic importance sites according to importance scoring in JRFR for H3N2 influenza data.

Antigenic drift events	Combination of mutations
HK68-EN72	S193N-G144D
EN72-VI75	N53D-S193D-S145N
VI75-TX77	S137G
TX77-BK79	D144V-N2K
BK79-SI87	Y155H-K189R
SI87-BE89	N145K, N145K-G135E, N145K-N193S
BE89-BE92	K145N-E156K-R189S, K145N-E156K-T262N-R189S, K145N-E156K-S133D-R189S
BE92-WU95	K135T-N145K-L226V, K135T-N145K-N262S
WU95-SY97	V196A-N276K-E158K-K156Q, V196A-N276K-E158K-K156Q-K62E
SY97-FU02	A131T-H155T-V202I

Table 4. Multiple mutations driving 10 antigenic drifts for H3N2 influenza viruses inferred by JRFR.

For example, the reduction seen in H3N2 virus binding to red blood cells^{26,27} can lead to problems performing and interpreting HI assays. Furthermore, because antigenic characterization is relatively labor-intensive, only a small portion (generally, fewer than 20%) of the influenza isolates sequenced will be antigenically characterized.

With the development of sequencing techniques, influenza protein sequencing has become a routine for influenza studies. Many newly sequenced influenza protein sequences have been stored in influenza databases like NCBI influenza database¹⁵. Much of the burden for influenza surveillance could be avoided if reliable sequence-based antigenic prediction methods can be established. JRFR produces relative low prediction error and reasonable antigenic cartography, which could serve as an initial screen of antigenic variants for further experimental analyses.

In the JRFR framework, we systematically evaluated the powers of 95 amino acids substitution matrices in predicting influenza antigenicity, which reflecting various physicochemical and biochemical properties of amino acids. We found that structure-based features outperformed all other features, followed by amino acids hydrophobicity. The importance of HA structure in influenza antigenicity has long been identified²⁸. Interestingly, commonly used substitution matrices including binary matrix, PAM250 and BLOSUM62 are not performing well, suggesting the necessity of combining protein structure information in studies to predict phenotypes using protein sequences. By combining a few feature matrices, the prediction accuracy could be further improved, indicating that influenza antigenicity might be determined by multiple factors, though HA structure might play dominant roles.

In addition, we inferred 34 antigenically important protein sites, most of which are located at the 5 epitopes, especially in epitope A and B. Ndifon *et al.*²⁹ presented a competitive model to predict antibody escape and proposed that antigenic drift events would be associated with amino acid changes that occur in epitopes with high neutralization efficiencies (i.e., epitopes A, B, and D) rather than in those with low neutralization efficiencies (i.e., epitopes C and E). The results are consistent with our findings. Meanwhile, we found that a small subset of amino

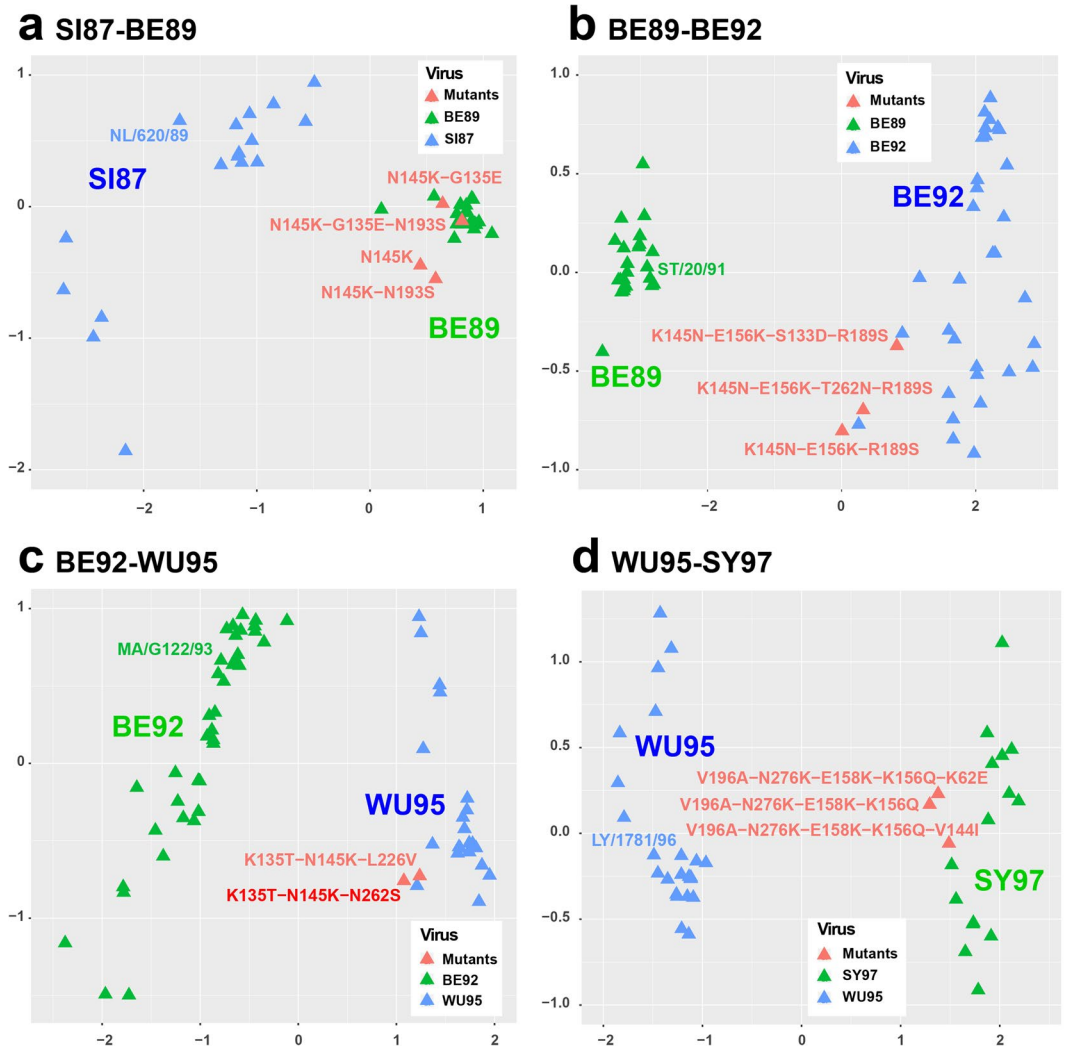


Figure 5. Antigenic cartographies to illustrate the key mutations driving the 4 antigenic drift events including (a) SI87-BE89, (b) BE89-BE92, (c) BE92-WU95, and (d) WU95-SY97.

acids mutations could drive most antigenic drift events for H3N2 influenza viruses, confirming the result from a few previous studies^{2,12}.

In the end, we would like to point out that our framework works generally for all influenza sub-types though we used H3N2 influenza as an illustration. In the future, we plan to predict the antigenicity of other sub-types like H1N1, H5N1 and H7N9, and compare their antigenically associated amino acid mutations or antigenic determinant regions. In addition, our method could also be applied to investigate other problems, such as disease and drug prediction, DNA-binding protein prediction³⁰, protein fold recognition³¹, detection of tubule boundary³², and other related problems^{33,34} etc. However, it is out of the scope of this study.

Materials and Methods

Influenza data. In this study, we adopted the H3N2 influenza data from Smith *et al.*⁵ which contains a partially revealed HI table consisting of 253 viruses and 79 vaccines from 1968 to 2003. There are 11 major antigenic clusters including HK68, EN72, VI75, TX77, BK79, SI87, BE89, BE92, WU95, SY97 and FU02, named by vaccine strain in the respective cluster⁵. We also downloaded the HA protein sequences of the 253 viruses and those of a total 1638 viruses available from NCBI flu database from 1968 to 2014. The HA protein sequences were aligned by MUSCLE²⁰, and we only kept the 329 sites belong to HA1 protein for further analyses.

The random forest algorithm. We applied the random forest algorithm to predict antigenic distances using 95 single amino acids substitution models³⁵. It is a nonlinear ensemble algorithm taking each non-conservative protein site as a feature and pair-wise antigenic distances among viruses as responses. Let n be the number of viruses ($n = 253$ for H3N2 data⁵) and S be the alignment of their HA1 sequences. Since conservative sites are non-informative, we removed them from S . Let m be the number of non-conservative sites ($m = 154$ for H3N2 data). Thus after removing conservative sites, S is an $n \times m$ (253×154 for H3N2 data) matrix with each entry being an amino acid.

Feature construction. We constructed the feature matrix \mathbf{X} as follows: Let \mathbf{S}_{ij} be the amino acid at position (i, j) in \mathbf{S} and \mathbf{X}_j be the j^{th} column of \mathbf{X} . Then $\mathbf{X}_j = \{D_{S_{ij}, S_{lj}}\}$, a vector traversing all ordered pairs of (k, l) with $1 \leq k \leq l \leq n$. Clearly, \mathbf{X}_j is a vector of length $N = \binom{n}{2}$ and \mathbf{X} is an $N \times m$ matrix. Here, $\mathbf{D}_{a,b}$ denotes the dissimilarity between amino acids a and b . It is of note that AAindex only provides similarity matrix \mathbf{A} among amino acids. We transformed \mathbf{A} into dissimilarity matrix \mathbf{D} using the following formula,

$$\mathbf{D}_{a,b} = (\mathbf{A}_{a,a} + \mathbf{A}_{b,b}) - 2\mathbf{A}_{a,b}. \quad (1)$$

Response. We adopted antigenic distance proposed by Smith *et al.*⁵ as our response \mathbf{y} , where \mathbf{y} consists of all distances between ordered pairs of viruses. Clearly, \mathbf{y} is also of length N . Given an HI table of n viruses, \mathbf{y} could be calculated directly from the website provided in ref. 5.

After the feature matrix \mathbf{X} and the response vector \mathbf{y} were constructed, we applied the random forest function in R package 'randomForest' to construct the prediction model³⁶. We set the bootstrapping (tree) number to be 500 and the number of features to be $\frac{m}{4}$ for each tree. We then tested and compared the 95 dissimilarity matrices based on a 10-fold cross-validation process and used root-mean-square error (RMSE) to evaluate their performances, which are described as follows.

RMSE. Let $\alpha = (\alpha_1, \alpha_2, \dots, \alpha_N)$ and $\beta = (\beta_1, \beta_2, \dots, \beta_N)$ be two prediction vectors, then the RMSE between α and β is defined as

$$\text{RMSE}(\alpha, \beta) = \sqrt{\frac{\sum_{i=1}^N (\alpha_i - \beta_i)^2}{N}} \quad (2)$$

Accuracy and specificity. For a pair of viruses with underlying antigenic distance y , we define them to be true antigenic variants if $y \geq 2$, and false otherwise. Similar they are called positive antigenic variants if the predicted antigenic distance $\hat{y} \geq 2$ by JRFR, and negative otherwise. By this way, we can define true positive (TP) pairs (i.e., $y \geq 2$ and $\hat{y} \geq 2$), false positive (FP) ($y < 2$ and $\hat{y} \geq 2$), true negative (TN) ($y < 2$ and $\hat{y} < 2$), and false negative (FN) ($y \geq 2$ and $\hat{y} < 2$). The accuracy of a method is defined as

$$\text{accuracy} = \frac{TP + TN}{TP + FP + TN + FN} \quad (3)$$

and the specificity is defined as

$$\text{specificity} = \frac{TN}{TN + FP}. \quad (4)$$

10-fold cross-validation. We divided \mathbf{y} randomly into 10 equal parts, 9 parts of which (with the corresponding sub-matrices of \mathbf{X}) are used for training and the remaining one part for prediction. The process is repeated for 10 times until each part is used as the prediction set once. By merging the prediction results for each part, we obtained a prediction vector $\hat{\mathbf{y}}$. The RMSE between \mathbf{y} and $\hat{\mathbf{y}}$ was used to tune model parameters and compare the performances of different models.

The JRFR algorithm. In the JRFR algorithm, we combined multiple feature matrices (derived from different amino acid similarity matrices in AAindex¹⁸) to construct decision trees in random forest algorithm. Specifically, let $\mathbf{X}^{(1)}, \mathbf{X}^{(2)}, \dots, \mathbf{X}^{(k)}$ be k feature matrices, each consisting of m features corresponding to m non-conservative sites in HA1. We set one of the feature matrices, say $\mathbf{X}^{(1)}$ to be the main matrix and other to be auxiliary ones. For each auxiliary matrix $\mathbf{X}^{(i)}$ with $2 \leq i \leq k$, we then applied an linear regression process to remove its overlapping information from the main matrix as follows: let $\mathbf{X}_j^{(i)}$ and $\mathbf{X}_j^{(1)}$ be the j^{th} feature vectors of $\mathbf{X}^{(i)}$ and $\mathbf{X}^{(1)}$ respectively. There exist constants α_{ij}, β_{ij} , and vector ε_{ij} such that

$$\mathbf{X}_j^{(i)} = \alpha_{ij} + \beta_{ij}\mathbf{X}_j^{(1)} + \varepsilon_{ij} \quad (5)$$

where α_{ij} is the intercept, β_{ij} is the regression coefficient and ε_{ij} is the residual vector. We constructed a new feature matrix with each feature vector being ε_{ij} for $1 \leq j \leq m$. For brevity, we still used $\mathbf{X}^{(i)}$ to represent this matrix for $2 \leq i \leq k$. By this way, we obtained new $k - 1$ auxiliary matrices independent of $\mathbf{X}^{(1)}$.

We then combined the main feature matrix and new auxiliary ones to predict antigenic distance using random forest algorithm. That is, we extended the number of features to $k \times m$, and applied the usual random forest process introduced above. In practice, we only used the top 15 feature matrices (as ranked in Supplementary Table S1) as main feature matrices and restricted the number of auxiliary feature matrices to be less than 2. Similar to single feature matrix analysis, we set the bootstrapping (tree) number to be 500 and the number of features to be $\frac{k \times m}{4}$ for each tree.

Importance score. To calculate the importance of a feature, the random forest algorithm permutes the values of this feature. It then calculates and normalizes the difference of out-of-bag error before and after permutation³⁵. By applying the random forest function in R, we obtained importance scores for features in both main feature matrix

and auxiliary ones. Let $I_j^{(i)}$ be the importance score of the j^{th} feature in the main feature matrix and $I_j^{(i)}$ with $2 \leq i \leq k$ be its importance scores in auxiliary feature matrices. Since the j^{th} feature in both main matrix and auxiliary ones represents information from the j^{th} non-conservative site in HA1 sequence, we defined the importance of the j^{th} non-conservative site to be $\frac{\sum_{i=1}^k I_j^{(i)}}{k}$.

Building the JRFR prediction model. We sorted all non-conservative sites in descending order based on their importance scores, and selected site one by one from top to join the JRFR algorithm, until the best 10-fold cross-validation RMSE is obtained. For H3N2 data, we selected the top 85 sites to building the final JRFR model by this process.

Construction of antigenic and genetic cartography. The antigenic map was directly constructed from the predicted antigenic distance matrix among viruses using classical multidimensional scaling (MDS). To construct the genetic map, we first calculated the p-distance matrix between pair of viruses and then applied classical MDS.

References

1. WHO. influenza(seasonal). *Fact sheet* No 211 (2014).
2. Sun, H. *et al.* Using sequence data to infer the antigenicity of influenza virus. *MBio* 4(4), e00230–13, doi:10.1128/mBio.00230-13 (2013).
3. Blackburne, B. P., Hay, A. J. & Goldstein, R. A. Changing selective pressure during antigenic changes in human influenza h3. *PLoS Pathogens* 4(5), e1000058, doi:10.1371/journal.ppat.1000058 (2008).
4. CDC. *CDC admits flu shots fail half the time.* <http://www.nvcc.org/nvcc-vaccine-news/april-2016/cdc-admits-flu-shots-fail-half-the-time.aspx>.
5. Smith, D. J. *et al.* Mapping the antigenic and genetic evolution of influenza virus. *Science* 305(5682), 371–376, doi:10.1126/science.1097211 (2004).
6. Hirst, G. K. Studies of antigenic differences among strains of influenza a by means of read cell agglutination. *The Journal of Experimental Medicine* 78(5), 407–423, doi:10.1084/jem.78.5.407 (1943).
7. Bao, Y. *et al.* The influenza virus resource at the national center for biotechnology information. *Journal of Virology* 82(2), 596–601, doi:10.1128/JVI.02005-07 (2008).
8. Barnett, J. L., Yang, J., Cai, Z., Zhang, T. & Wan, X. F. Antigenmap 3d: an online antigenic cartography resource. *Bioinformatics* 28, 1292–1293, doi:10.1093/bioinformatics/bts105 (2012).
9. Lee, M. S. & Chen, J. S. Predicting antigenic variants of influenza a/h3n2 viruses. *Emerging Infectious Diseases* 10(8), 1385–1390, doi:10.3201/eid1008.040107 (2004).
10. Liao, Y. C., Lee, M. S., Ko, C. Y. & Hsiung, C. A. Bioinformatics models for predicting antigenic variants of influenza a/h3n2 virus. *Bioinformatics* 24, 505–512, doi:10.1093/bioinformatics/btm638 (2008).
11. Wang, W., DeFeo, C. J., Alvarado-Facundo, E., Vassell, R. & Weiss, C. D. Intermonomer interactions in hemagglutinin subunits ha1 and ha2 affecting hemagglutinin stability and influenza virus infectivity. *Journal of Virology* 89(20), 10602–10611, doi:10.1128/JVI.00939-15 (2015).
12. Yang, J., Zhang, T. & Wan, X. F. Sequence-based antigenic change prediction by a sparse learning method incorporating co-evolutionary information. *PLoS One* 20, 317–330 (2009).
13. Qiu, J., Qiu, T., Yang, Y., Wu, D. & Cao, Z. Incorporating structure context of ha protein to improve antigenicity calculation for influenza virus a/h3n2. *Scientific Reports* 6, 31156, doi:10.1038/srep31156 (2016).
14. Neher, R. A., Bedford, T., Daniels, R. S., Russell, C. A. & Shraiman, B. I. Prediction, dynamics, and visualization of antigenic phenotypes of seasonal influenza viruses. *Proceedings of the National Academy of Sciences of the United States of America* 113, E1701–1709, doi:10.1073/pnas.1525578113 (2016).
15. Huang, J. W., King, C. C. & Yang, J. M. Co-evolution positions and rules for antigenic variants of human influenza a/h3n2 viruses. *BMC Bioinformatics* 10 (Suppl 1), S41, doi:10.1186/1471-2105-10-S1-S41 (2009).
16. Ren, X. *et al.* Computational identification of antigenicity-associated sites in the hemagglutinin protein of a/h1n1 seasonal influenza virus. *PLoS One* 10(5), e0126742, doi:10.1371/journal.pone.0126742 (2015).
17. Cai, Z. *et al.* Identifying antigenicity-associated sites in highly pathogenic h5n1 influenza virus hemagglutinin by using sparse learning. *Journal of Molecular Biology* 422(1), 145–55, doi:10.1016/j.jmb.2012.05.011 (2012).
18. Kawashima, S. *et al.* Aaindex: amino acid index database, progress report 2008. *Nucleic Acids Research* 36 (Database issue), D202–e0205 (2008).
19. Touw, W. G. *et al.* Data mining in the life sciences with random forest: a walk in the park or lost in the jungle? *Briefings in Bioinformatics* 14(3), 315–26, doi:10.1093/bib/bbs034 (2013).
20. Edgar, R. Muscle: multiple sequence alignment with high accuracy and high throughput. *Nucleic Acids Research* 32(5), 1792–1797, doi:10.1093/nar/gkh340 (2004).
21. Wiley, D. C., Wilson, I. A. & Skehel, J. J. Structural identification of the antibody-binding sites of hong kong influenza haemagglutinin and their involvement in antigenic variation. *Nature* 289, 373–378, doi:10.1038/289373a0 (1981).
22. Wilson, I. A. & Cox, N. Structural basis of immune recognition of influenza virus hemagglutinin. *Annual Review of Immunology* 8, 737–787, doi:10.1146/annurev.iy.08.040190.003513 (1990).
23. Kilbourne, E. D. Future influenza vaccines and the use of genetic recombinants. *Bulletin of the World Health Organisation* 41(3), 643–645 (1969).
24. Chambers, B., Parkhouse, K., Ross, T., Alby, K. & Hensley, S. Identification of hemagglutinin residues responsible for h3n2 antigenic drift during the 2014? 015 influenza season. *Cell Reports* 12(1), 1–6, doi:10.1016/j.celrep.2015.06.005 (2015).
25. Koel, B. F., Burke, D. F., Bestebroer, T. M. & Vliet, S. Substitutions near the receptor binding site determine major antigenic change during influenza virus evolution. *Science* 342(6161), 976–979, doi:10.1126/science.1244730 (2013).
26. Morishita, T., Nobusawa, E. & Nakajima, S. Studies on the molecular basis for loss of the ability of recent influenza a (h1n1) virus strains to agglutinate chicken erythrocytes. *Journal of General Virology* 77, 2499–2506, doi:10.1099/0022-1317-77-10-2499 (1996).
27. Nobusawa, E. *et al.* Change in receptor-binding specificity of recent human influenza a viruses (h3n2): A single amino acid change in hemagglutinin altered its recognition of sialyloligosaccharides. *Virology* 278(2), 587–596, doi:10.1006/viro.2000.0679 (2000).
28. Wilson, I. *et al.* The structure of an antigenic determinant in a protein. *Cell* 37(3), 767–778 (1984).
29. Ndifon, W., Wingreen, N. S. & Levin, S. A. Differential neutralization efficiency of hemagglutinin epitopes, antibody interference, and the design of influenza vaccines. *Proceedings of the National Academy of Sciences of the United States of America* 106, 8701–8706, doi:10.1073/pnas.0903427106 (2009).
30. Wei, L., Tang, J. & Zou, Q. Local-DPP: An improved DNA-binding protein prediction method by exploring local evolutionary information. *Information Sciences* 384, 135–144, doi:10.1016/j.ins.2016.06.026 (2017).

31. Wei, L. & Zou, Q. Recent Progress in Machine Learning-Based Methods for Protein Fold Recognition. *International Journal of Molecular Sciences* **17**(12), 2118, doi:[10.3390/ijms17122118](https://doi.org/10.3390/ijms17122118) (2016).
32. Su, R. *et al.* Detection of tubule boundaries based on circular shortest path and polar-transformation of arbitrary shapes. *Journal of microscopy* **264**(2), 127–142, doi:[10.1111/jmi.2016.264.issue-2](https://doi.org/10.1111/jmi.2016.264.issue-2) (2016).
33. Wei, L., Xing, P., Shi, G., Ji, Z. L. & Zou, Q. Fast prediction of protein methylation sites using a sequence-based feature selection technique. *IEEE/ACM Transactions on Computational Biology and Bioinformatics*, doi:[10.1109/TCBB.2017.2670558](https://doi.org/10.1109/TCBB.2017.2670558) (2017).
34. Wei, L., Xing, P., Tang, J. & Zou, Q. PhosPred-RF: a novel sequence-based predictor for phosphorylation sites using sequential information only. *IEEE Transactions on Nanobioscience*, doi:[10.1109/TNB.2017.2661756](https://doi.org/10.1109/TNB.2017.2661756) (2017).
35. Liaw, A. & Wiener, M. Classification and regression by randomforest. *R News* **20**, 317–330 (2009).
36. Liaw, A. & Wiener, M. *Package randomForest*. <https://www.stat.berkeley.edu/~breiman/RandomForests/>.

Acknowledgements

This work was partially supported by the National Natural Science Foundation of China (No. 61272312) and the 521 Talent Cultivation Plan of Zhejiang Sci-Tech University.

Author Contributions

J.L.Y. and Y.Z. conceived and designed the experiments. Y.Y., X.L. and B.L. performed the experiments and analysed the data. J.L.Y., X.L. and Y.Z. wrote the paper. Y.Y., B.L., L.H., P.H., F.W., J.S.Y., H.S. contribute to the discussion, and helped to revise the paper.

Additional Information

Supplementary information accompanies this paper at doi:[10.1038/s41598-017-01699-z](https://doi.org/10.1038/s41598-017-01699-z)

Competing Interests: The authors declare that they have no competing interests.

Publisher's note: Springer Nature remains neutral with regard to jurisdictional claims in published maps and institutional affiliations.



Open Access This article is licensed under a Creative Commons Attribution 4.0 International License, which permits use, sharing, adaptation, distribution and reproduction in any medium or format, as long as you give appropriate credit to the original author(s) and the source, provide a link to the Creative Commons license, and indicate if changes were made. The images or other third party material in this article are included in the article's Creative Commons license, unless indicated otherwise in a credit line to the material. If material is not included in the article's Creative Commons license and your intended use is not permitted by statutory regulation or exceeds the permitted use, you will need to obtain permission directly from the copyright holder. To view a copy of this license, visit <http://creativecommons.org/licenses/by/4.0/>.

© The Author(s) 2017